J Appl Physiol 115: 383–393, 2013.
First published May 23, 2013; doi:10.1152/japplphysiol.01415.2012.

Endocardial endothelium is a key determinant of force-frequency relationship in rat ventricular myocardium

Xiaoxu Shen,[1,2,5] Zhen Tan,[3] Xin Zhong,[4] Ye Tian,[4] Xian Wang,[1] Bo Yu,[5] Genaro Ramirez-Correa,[6] Anne Murphy,[6] Kathleen Gabrielson,[7] Nazareno Paolocci,[8] and Wei Dong Gao[2]

[1]*Cardiology Department, Dongzhimen Hospital Affiliated to Beijing University of Chinese Medicine, Beijing, China;* [2]*Department of Anesthesiology and Critical Care Medicine, Johns Hopkins University School of Medicine, Baltimore, Maryland;* [3]*Department of Cardiology, 4th Teaching Hospital, Harbin Medical University, Harbin, China;* [4]*Department of Cardiology and Pathophysiology, 2nd Teaching Hospital, Harbin Medical University, Harbin, China;* [5]*Department of Cardiology, 2nd Teaching Hospital, Harbin Medical University, Harbin, China;* [6]*Department of Pediatrics, Johns Hopkins University School of Medicine, Baltimore, Maryland;* [7]*Department of Molecular and Comparative Pathobiology, Johns Hopkins University School of Medicine, Baltimore, Maryland; and* [8]*Department of Medicine, Johns Hopkins University School of Medicine, Baltimore, Maryland*

Submitted 26 November 2012; accepted in final form 10 May 2013

Shen X, Tan Z, Zhong X, Tian Y, Wang X, Yu B, Ramirez-Correa G, Murphy A, Gabrielson K, Paolocci N, Gao WD. Endocardial endothelium is a key determinant of force-frequency relationship in rat ventricular myocardium. *J Appl Physiol* 115: 383–393, 2013. First published May 23, 2013; doi:10.1152/japplphysiol.01415.2012.—We tested the hypothesis that removing endocardial endothelium (EE) negatively impacts the force-frequency relationship (FFR) of ventricular myocardium and dissected the signaling that underlies this phenomenon. EE of rat trabeculae was selectively damaged by brief (<1 s) exposure to 0.1% Triton X-100. Force, intracellular Ca^{2+} transient (iCa^{2+}), and activity of protein kinase A (PKA) and protein kinase C (PKC) were determined. In control muscles, force and iCa^{2+} increased as the stimulation frequency increased in steps of 0.5 Hz up to 3.0 Hz. However, EE-denuded (EED) muscles exhibited a markedly blunted FFR. Neither isoproterenol (ISO; 0.1–5 nmol/l) nor endothelin-1 (ET-1; 10–100 nmol/l) alone restored the slope of FFR in EED muscles. Intriguingly, however, a positive FFR was restored in EED preparations by combining low concentrations of ISO (0.1 nmol/l) and ET-1 (20 nmol/l). In intact muscles, PKA and PKC activity increased proportionally with the increase in frequency. This effect was completely lost in EED muscles. Again, combining ISO and ET-1 fully restored the frequency-dependent rise in PKA and PKC activity in EED muscles. In conclusion, selective damage of EE leads to significantly blunted FFR. A combination of low concentrations of ISO and ET-1 successfully restores FFR in EED muscles. The interdependence of ISO and ET-1 in this process indicates cross-talk between the β_1-PKA and ET-1-PKC pathways for a normal (positive) FFR. The results also imply that dysfunction of EE and/or EE-myocyte coupling may contribute to flat (or even negative) FFR in heart failure.

endocardial endothelium; cardiac excitation-contraction coupling; force-frequency relationship; isoproterenol; endothelin-1; rat myocardium

CARDIAC ENDOTHELIAL CELLS have an obligatory role in heart growth and performance (9). The interaction between endothelial cells and myocytes, also known as cardiac endothelial-myocardial signaling, influences cardiac contraction and force development. The selective removal of endocardial endothelium (EE) decreases the magnitude, time to peak, and rate of force development and abbreviates contraction (10, 56). Interestingly, the adverse effects are reversible with an unknown endothelial contraction-prolonging factor (56) or endothelin-1 (ET-1) (62). One mechanism for cardiac endothelium to modulate contraction is to maintain normal myofilament Ca^{2+} responsiveness via autocrine and paracrine signaling from endothelial cells (9). In this sense, agents such as nitric oxide (NO), ET-1, prostacyclin (PGI_2), and angiotensin II are critically involved. For instance, ET-1 is a potent positive inotropic agent (41, 42) that increases myofilament Ca^{2+} responsiveness (63). Its positive inotropic effect requires activation of both protein kinase C (PKC) and protein kinase A (PKA) (11).

Another important feature of myocardial contraction is the dependency of force generation on the imposed frequency, known as the force-frequency relationship (FFR). Under physiological conditions, most, if not all, mammalian myocardia exhibit a positive FFR with stimulation between 0.5 and 3.0 Hz (22). Central to this phenomenon is the increase in intracellular Ca^{2+} (21) that results from *1*) increased Ca^{2+} entry via L-type Ca^{2+} channels (57) and increased uptake and release of Ca^{2+} by the sarcoplasmic reticulum (SR) (29); and *2*) increased intracellular Na^+, which promotes Ca^{2+} entry via Na^+/Ca^{2+} exchange (39). Thus a positive FFR is tightly regulated by all factors and signaling that control the activities of sarcolemmal L-type Ca^{2+} channels, SR Ca^{2+}-ATPase, and the Na^+/Ca^{2+} exchanger (22). These, in turn, are affected by the calmodulin kinase system (39). The presence of phospholamban is also important for a positive FFR (7). Perturbation at any of these levels would affect intracellular Ca^{2+} availability, dampening the effects of FFR. For example, one of the adverse features of heart failure, in which Ca^{2+} handling is severely impaired, is markedly blunted or null FFR enhancement of force generation (7, 13, 23, 53).

FFR is generally believed to be an intrinsic property of the myocyte. Yet, given the tight coupling between endothelial cell and myocyte and the fact that endothelins have a profound impact on basal myocardial contraction (9, 50), it is conceivable that intact EE function chiefly contributes to a positive FFR. For example, isolated cardiac muscles with intact endothelium exhibited robust positive FFR (i.e., 2- to 4-fold increases in force development) when stimulation rate increased

Address for reprint requests and other correspondence: W. D. Gao, Dept. of Anesthesiology and Critical Care Medicine, The Johns Hopkins Univ. School of Medicine, 1800 Orleans St., Zayed Tower 6208, Baltimore, MD 21287 (e-mail: wgao3@jhmi.edu).

8750-7587/13 Copyright © 2013 the American Physiological Society

Downloaded from www.physiology.org/journal/jappl (071.179.232.088) on January 25, 2020.

from 0.5 Hz to 2.0–4.0 Hz (27, 35, 40, 46, 60). However, no study has investigated the direct involvement of EE in FFR. Therefore, we tested the hypothesis that intact endothelium is essential for a fully developed positive FFR in rat cardiac muscle. We also started dissecting the signaling pathways that possibly connect changes in stimulation frequency to increased force generation via EE, focusing in particular on PKA and PKC signaling.

MATERIALS AND METHODS

Animals

LBN/F1 rats (250–300 g, Harlan Laboratories, Indianapolis, IN) were used in these experiments. Animal care and experimental protocols were approved by the Animal Care and Use Committee of The Johns Hopkins University School of Medicine.

Trabecular Muscle Preparation

The rats were anesthetized by intra-abdominal injection with pentobarbital sodium (100 mg/kg); the heart was exposed by midsternotomy, rapidly excised, and placed in a dissection dish. The aorta was cannulated and the heart perfused in a retrograde fashion (~15 ml/min) with dissecting Krebs-Henseleit (K-H) solution equilibrated with 95% O_2-5% CO_2. The dissecting K-H solution was composed of (in mmol/l) 120 NaCl, 20 $NaHCO_3$, 5 KCl, 1.2 MgCl, 10 glucose, 0.5 $CaCl_2$, and 20 2,3-butanedione monoxime (BDM) [pH 7.35–7.45 at room temperature (21–22°C)]. Trabecular muscle from the right ventricle of the heart was dissected and mounted between a force transducer and a motor arm, superfused with K-H solution without BDM at a rate of ~10 ml/min, and stimulated at 0.5 Hz. Unless otherwise specified, all experiments were performed at an external Ca^{2+} concentration of 0.5 mM.

Force was measured by a force transducer system (KG7, Scientific Instruments, Heidelberg, Germany) and expressed in millinewtons per square millimeter of cross-sectional area. The muscles underwent isometric contractions with the resting muscle length set such that resting force was 15% of total force development (i.e., optimal muscle length). This resting muscle length, corresponding to a resting sarcomere length of 2.20–2.30 μm as determined by laser diffraction (26), was maintained throughout the experiments. All experiments were carried out at room temperature (20–22°C).

Measurement of Intracellular Ca^{2+} Concentration ($[Ca^{2+}]_i$)

$[Ca^{2+}]_i$ was measured by using the free acid form of fura-2 as described in previous studies (14, 25). Fura-2 potassium salt was microinjected iontophoretically into one cell and allowed to spread throughout the whole muscle (via gap junctions). The tip of the electrode (~0.2 μm in diameter) was filled with fura-2 salt (1 mmol/l), and the remainder of the electrode was filled with 150 mM KCl. After the electrode was successfully impaled into a superficial cell in nonstimulated muscle, a hyperpolarizing current of 5–10 nA was passed continuously for ~15 min. In some muscles, multiple injections (up to 3–4) were applied at different sites, with duration of the injection limited to <10 min at each site to achieve an optimal signal-to-noise ratio. As previously established, this loading did not affect force development (23, 24). Fura-2 epifluorescence was measured by excitation at 380 and 340 nm. Fluorescent light was collected at 510 nm by a photomultiplier system (PTI, Birmingham, NJ). The output of the photomultiplier was collected and digitized. $[Ca^{2+}]_i$ was given by the following equation (after subtraction of the autofluorescence):

$$\left[Ca^{2+}\right]_i = K_d\left(R - R_{min}\right)/\left(R_{max} - R\right) \qquad (1)$$

where R is the observed ratio of fluorescence (340 nm/380 nm), K_d is the apparent dissociation constant, R_{max} is the ratio of 340 nm/380 nm at saturating $[Ca^{2+}]$, and R_{min} is the ratio of 340 nm/380 nm at $[Ca^{2+}] = 0$. The values of K_d, R_{max}, and R_{min} were determined by in vivo calibrations as described previously (25).

Measurement of Action Potentials (APs)

Membrane potential was measured as described previously (15), except that we used glass microelectrodes that were somewhat stiffer. These fine electrodes were filled with 3 M KCl and connected to a high-input impedance amplifier (MEZ-8201, Nihon Kohden). The center of the trabecula was impaled. To ensure that we obtained stable measurements with these electrodes but did not cause local damage during contraction, we inhibited mechanical movements of muscle contraction with 5 mmol/l BDM. We were able to inhibit contraction by more than 70% without causing changes in the excitation process, as evidenced by the fact that Ca^{2+} transients changed little (2).

Removal of EE

EE surrounding the trabeculae was selectively destroyed by brief exposure (<1–2 s) to K-H solution containing 0.1% Triton X-100. Multiple investigators have shown that this protocol causes little myocardial damage (10, 56, 62). We chose trabecular muscles that were ~250 μm wide, ~80–100 μm thick, and 2,000 μm long. Based on these dimensions and the size of an individual myocyte (100 × 5 × 10 μm), ~1,500 myocytes are covered by EE (i.e., ~20–30% of myocytes in the specimen were in contact with EE).

We also verified that the muscles used in these experiments were not overtreated with Triton X-100, which leads to chemical skinning of the muscle. First, immunofluorescence imaging of the whole trabeculae was performed in selected control and EED muscles. These muscles were immediately fixed in 4% paraformaldehyde after treatment, washed three times in PBS, blocked in Image iT Enhancer (Invitrogen, Carlsbad, CA) for 30 min, and washed three more times in PBS. Then Alexa Fluor Oregon Green 488 WGA (5 μg/ml; Invitrogen) was added. After a 10-min incubation, the muscles were washed three times in PBS, permeabilized for 20 min in PBS-0.1% Triton X-100, washed three times in PBS, and incubated in Alexa Fluor 594 Phalloidin (Invitrogen) according to the manufacturer's instructions. After the muscles were washed three times in PBS, nuclei were counterstained with Hoechst 33342 (Pierce, Rockfort, IL) for 5 min according to the manufacturer's instructions, washed, and mounted in ProLong Gold Antifade (Invitrogen). Image stacks were acquired on a Zeiss AxioExaminer upright microscope with a 40×/1.1W LD C-Apo, water objective, with a 710NLO-Meta multiphoton and confocal module. Z stacks were processed for 3D reconstruction/visualization, and surface area was calculated. Endothelial nuclei intensities were analyzed with Imaris 6.4.2 (Bitplane Scientific Software). Second, we stained the muscles with Evan blue. Both control and Triton-treated muscles were fixed in buffered formalin solution (10%) and transferred to tissue cassettes. After being dehydrated in alcohol and washed, the samples were infiltrated with paraffin wax, sectioned, and then transferred onto glass slides. The images were viewed under a light microscope.

Determination of FFR

The FFR of individual muscles was measured by stimulating trabeculae in increments from 0.5 to 3.0 Hz. Each individual muscle was studied in a paired fashion: FFR was obtained before (control) and after EE removal. EE-denuded (EED) muscles were further divided into several experimental groups for FFR determinations: *1*) EED alone (untreated); *2*) EED muscle treated with isoproterenol (ISO), which had two subgroups, 0.1 nmol/l and 5 nmol/l. A baseline FFR was obtained and then the muscles were treated with ISO for 10 min before another FFR was obtained; *3*) EED muscle treated with endothelin 1 (ET-1), which had two subgroups, 20 μmol/l and 100 μmol/l. A baseline FFR was obtained and then the muscles were

Downloaded from www.physiology.org/journal/jappl (071.179.232.088) on January 25, 2020.

treated with ET-1 for 10 min before another FFR was obtained; *4*) EED muscle treated with a combination of 0.1 nmol/l ISO and 20 μmol/l ET-1; and *5*) EED muscle treated with PKA or PKC inhibitors. Two PKA pathway inhibitors (CGP, 2 μmol/l, and H-89, 1 μmol/l) and two PKC pathway inhibitors (neomycin, 10 μmol/l, and staurosporine, 10 nmol/l) were used. In these EED muscles, a baseline FFR was obtained, muscles were treated with a PKA or PKC inhibitor for 10 min, and then another FFR was obtained. A separate series of experiments was carried out for PKA and PKC activity determination (see below).

Measurement of PKA and PKC Activity

Tissue sample collection. The trabeculae were divided into four experimental groups. *Group 1* comprised control, intact trabeculae. We first determined the FFR by stimulating the muscle in increments from 0.5 to 3.0 Hz. Then we froze these muscles during stimulation at 0.5 or 3.0 Hz with specially crafted forceps whose tips had been immersed in liquid nitrogen. *Group 2* comprised untreated EED muscle. We first determined the FFR and then selectively damaged the EE. We then stimulated the muscle in increments from 0.5 to 3.0 Hz to determine the blunting of FFR. Muscles were flash frozen for collection as in the control group. In *group 3*, we treated EED muscles with low concentrations of ISO (0.1 nmol/l) and ET-1 (20 μmol/l) alone and in combination before stimulating them in increments from 0.5 to 3.0 Hz to determine FFR. Muscles were flash frozen for collection as in the control group. In *group 4*, we used inhibitors of PKA (H-89) or PKC (staurosporine). In one set, EED muscles were treated with H-89 (1 μmol/l) for 20 min before being exposed to ISO + ET-1. After confirming the block of positive FFR, the muscles were flash frozen for collection at 0.5 Hz and 3.0 Hz. In a second set, EED muscles were treated with ISO (0.1 nmol/l) first for 15 min, followed by staurosporine (10 nmol/l) for 15 min, before ET-1 (20 nmol/l) was added. The muscles were flash frozen at 0.5 Hz and 3.0 Hz after confirming the block of positive FFR. After being flash frozen with the forceps, all muscles were placed into liquid nitrogen and then stored at −80°C for later determination of PKA and PKC activity.

Tissue sample processing. Each sample was ground in liquid nitrogen and placed in RIPA lysis buffer [25 mM Tris-HCl, 150 mM NaCl, 1% NP-40, 1% sodium deoxycholate, 0.1% SDS (pH 7.6)]. Samples were then sonicated at 4°C. The protein concentrations were determined by using the Bio-Rad DC protein assay. We adjusted the protein content in all samples to 0.74–0.84 mg/ml to facilitate the kinase activity assays.

Kinase assay. We measured myocardial tissue PKA and PKC activity using kinase assay kits from Enzo Life Sciences (Plymouth Meeting, PA). The PKA/PKC activity assay is based on a solid-phase, enzyme-linked immunosorbent assay (ELISA) that utilizes a specific synthetic peptide as substrate for PKA/PKC and a polyclonal antibody (rabbit) that recognizes the phosphorylated form of the substrate. In our preliminary experiments, we determined that the amount of protein in our samples (0.80–1.90 mg/ml) was adequate for measurements of PKA and PKC activity. Briefly, at room temperature, the PKA or PKC substrate microtiter plate was soaked with kinase assay dilution buffer for 10 min. The processed samples were added to the appropriate wells of the plate. ATP was then added to wells to initiate the reaction. After incubation for 90 min at 30°C, the reaction was stopped by emptying each well. Then, phosphospecific substrate antibody was added to each well and incubated for 60 min. After the wells were washed, anti-rabbit IgG:HRP conjugate was added and

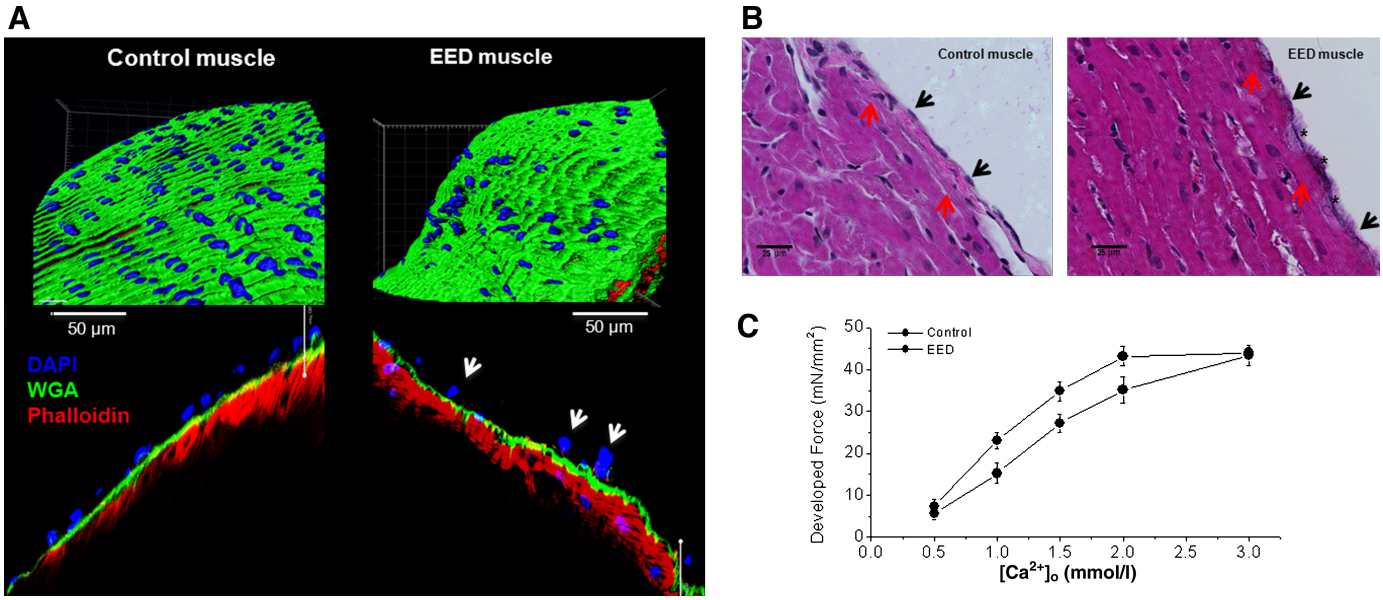

Fig. 1. Right ventricle rat trabeculae with intact and detergent-denuded endothelium. *A*: immunofluorescent images of trabecular muscles. *Top left*: intact/control trabecula shows 209 nuclei in the endocardial endothelium (EE) wrapping the muscle when normalized to total muscle area (i.e., $4.05 \times 10^3/\mu m^2$ of nuclear density). *Bottom left*: magnified images of a longitudinal section of the muscle showing components of the surface layer and underlying myocardium stained with Oregon Green 488 WGA (green for surface glycan), Hoechst 33342 (blue for cell nuclei), and Alexa Fluor 594 Phalloidin (red for α-sarcomeric actin). *Top right*: endocardial endothelium-denuded (EED) trabecula shows only 46 nuclei in the endocardial surface when normalized to the total muscle area (i.e., $8.31 \times 10^{-4}/\mu m^2$ of nuclear density). *Bottom right*: magnified image of the longitudinal section of an EED trabecula. Note the paucity of nuclei and the abnormal morphology (arrows) of those that remain, and the normal-appearing myocytes underneath. *B*: Evans blue staining of control (*left*) and EED (*right*) muscles. Control muscle showed intact EE with well-organized nuclei that were not stained by Evans blue (*black arrows*) and intact myocytes (*red arrows*). Note that in EED muscles, EE nuclei are absent, cell borders are ill-defined (*black arrows*), and Evans blue staining is evident (*black stars*). However, the underlying myocytes appear intact (*red arrows*). *C*: effect of external Ca^{2+} on force development before and after EE removal by Triton X-100. The muscles were first exposed to various concentrations of external Ca^{2+}, and twitch forces were recorded. Then, the same muscles were treated with Krebs-Henseleit solution containing 0.1% Triton X-100 (Ca^{2+} = 0.5 mmol/l) for less than ~1 s. After stabilization, the muscles were exposed to various external Ca^{2+} concentrations again. Note the full recovery of maximal twitch force after EE removal.

Downloaded from www.physiology.org/journal/jappl (071.179.232.088) on January 25, 2020.

incubated for 30 min. The wells were washed again, and stabilized tetramethylbenzidine substrate was added to each well. A 30- to 60-min incubation allowed full color development. The light absorbance was measured at 450 nm. Purified active PKA or PKC was diluted to 0.25 and 0.025 ng/μl to serve as positive controls. Kinase assay dilution buffer (without kinases) was used as the assay blank. The relative kinase activity was determined by the equation:

$$\text{Relative kinase activity} = \frac{\text{Absorbance (sample)} - \text{Absorbance (blank)}}{\text{Quantity of crude protein used } (\mu g)} \quad (2)$$

and its value was expressed as arbitrary units per microgram protein.

Statistical Analysis

Paired *t*-test, Student's *t*-test, and multivariate ANOVA were used for statistical analysis of the data (Systat 10.2.01; Systat Software, San Jose, CA). A value of $P < 0.05$ was considered to indicate significant differences between groups. Unless otherwise indicated, pooled data are expressed as means ± SE.

RESULTS

Removal of EE Markedly Blunts FFR in Isolated Rat Trabeculae

Muscles with selectively damaged EE appeared morphologically normal under light microscope and exhibited a 10–15% decrease in force development at baseline. We performed several experiments to illustrate that EE was successfully removed without damage to the underlying myocytes (Fig. 1). We stained some EED muscles with fluorescent dyes to display key structural components in the surface of the muscles (Fig. 1*A*). As evidenced by blue-colored endothelial nuclei, over 75–80% of endothelial cells were removed from the EED muscle, and the remaining cells exhibited abnormal morphology. The surface glycans (green) and the underlying myocytes (red) remained intact. We also stained the muscles with Evans blue. Evans blue, owing to its highly charged state, stains only damaged cells. There was persistent staining of the endocardial surface of the EED muscle, suggesting that the EE was damaged/removed. However, Evans blue did not stain the underlying myocytes (Fig. 1*B*). Finally, we compared maximal twitch force development before and after EE removal because maintained maximal twitch force would suggest no loss of myocytes after Triton treatment. After EE removal, EED muscles responded to external Ca^{2+} in a concentration-dependent manner similar to that observed before EE removal and, except for a higher requirement for external Ca^{2+}, the maximal twitch force was maintained as before EE removal (Fig. 1*C*), indicating that myocytes were undamaged by EE removal.

Intact rat cardiac trabecular muscle exhibited a positive FFR at room temperature and an external Ca^{2+} concentration of 0.5 mmol/l in the stimulation rate range of 0.5–3.0 Hz (Fig. 2). The positive FFR was accompanied by a positive Ca^{2+}-frequency relationship, suggesting that the positive FFR was the result of intracellular Ca^{2+} transients (iCa^{2+}) increasing as stimulation frequency increased. These observations are fully consistent with those of previous studies conducted at even higher temperatures (30°C and 37.5°C) (32, 60). The selective removal of EE blunted, but did not abolish the positive FFR staircase and increase in iCa^{2+}. In endothelium-intact preparations, systolic force increased by 243 ± 35% when stimulation frequency was increased from 0.5 to 3.0 Hz. After EE removal, systolic force increased by only 110 ± 28% ($P < 0.05$; Fig. 3*A*) over the same stimulation frequency range. Consistent with this finding, the increase in iCa^{2+} diminished from 165 ± 25% in EE-intact

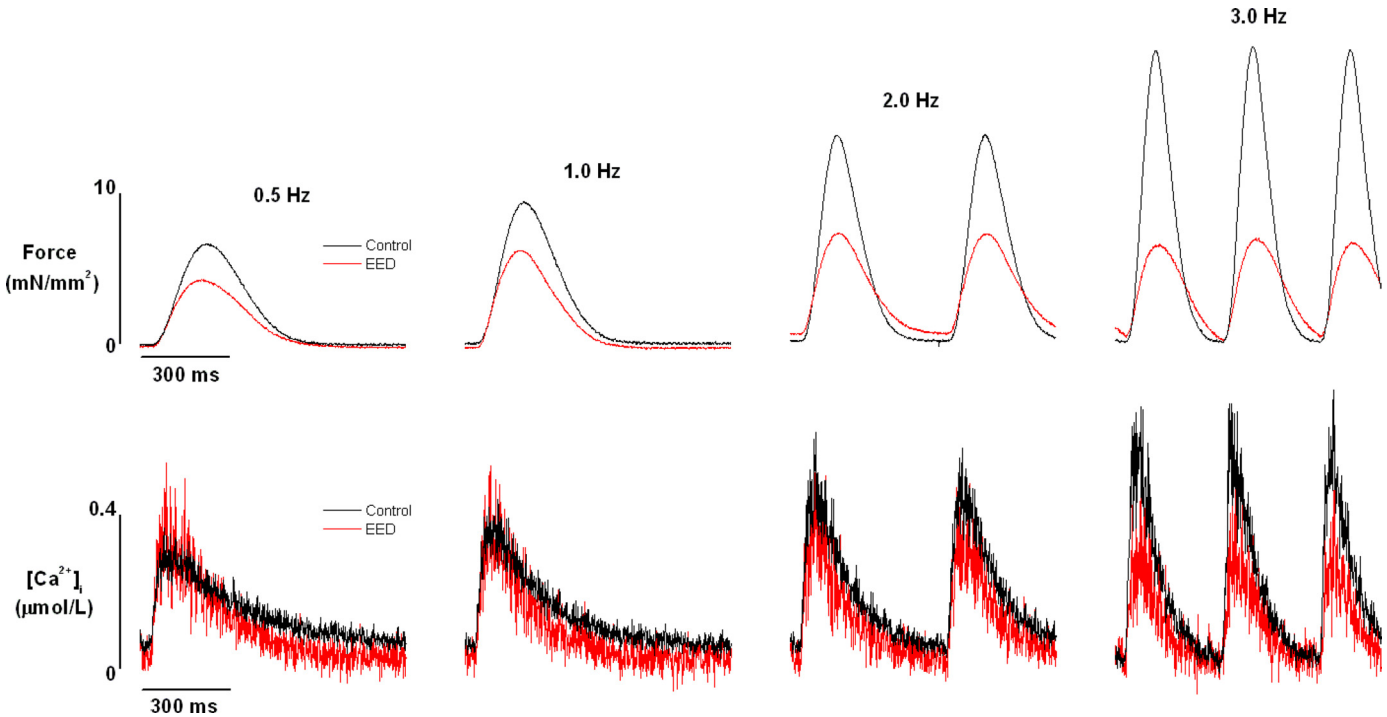

Fig. 2. Raw recordings of force (top panels) and corresponding intracellular Ca^{2+} transients (bottom panels) of trabeculae before and after endocardial endothelium denudation (EED) with 0.1% Triton X-100. Trabeculae were superfused with Krebs-Henseleit solution and stimulated at the frequencies shown. Experimental conditions: external $[Ca^{2+}] = 0.5$ mmol/l, temperature = 22°C.

Downloaded from www.physiology.org/journal/jappl (071.179.232.088) on January 25, 2020.

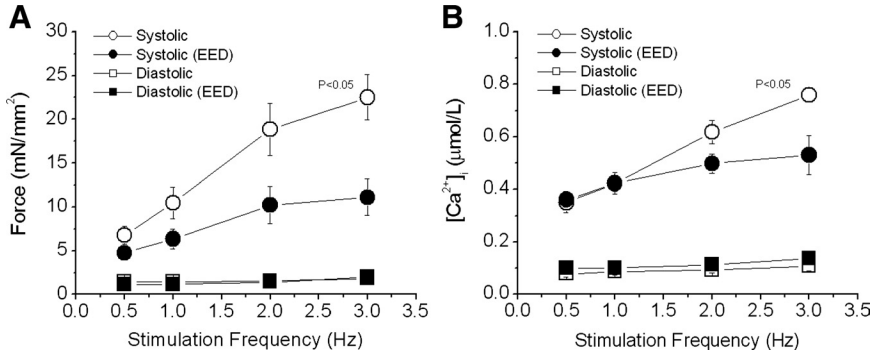

Fig. 3. Pooled data of the effect of EED on force-frequency relationship in rat trabeculae. Both systolic force (*A*) and intracellular Ca^{2+} transients (*B*) were suppressed as stimulation rate increased in EED muscles. Diastolic force and Ca^{2+} were not significantly affected. $P < 0.05$, control vs. EED groups, multivariate ANOVA, $n = 7$.

muscles to 47 ± 10% in EED muscles ($P < 0.05$; Fig. 3*B*). It should be mentioned that removal of EE resulted in an approximately 15% decrease in force development with little effect on Ca^{2+} transient at baseline. Diastolic force and Ca^{2+} were not affected by EE removal or by changes in stimulation frequency.

Prolongation of the AP contributes to positive FFR (57). To examine whether the flattened FFR after EE removal was due to AP shortening, we measured membrane APs in trabeculae before and after EE removal. Consistent with results of previous studies (48), AP duration was significantly prolonged by 15–25% after EE removal at the base stimulation rate of 0.5 Hz ($P < 0.05$ by paired *t*-test; Fig. 4). However, increasing the stimulation rate did not produce any appreciable difference in AP duration, either before or after EE removal. Thus changes in AP duration did not contribute to the flattened FFR response after EE removal.

Neither ISO nor ET-1 Alone Restores Positive FFR Staircase in EED Muscles

Another factor that affects the characteristics of FFR is Ca^{2+} release from the SR (manifested as iCa^{2+}). We found that the frequency-dependent increases in iCa^{2+} were attenuated in EED muscles. Therefore, we attempted to restore the steepness of the positive FFR in these muscles with ISO, a β-receptor agonist that increases SR Ca^{2+} release. A low concentration of ISO (0.1 nmol/l) did not affect force development, FFR (Fig. 5*A*), or iCa^{2+}. Higher doses (5–10 nmol/l) increased force and iCa^{2+} significantly but did not increase the steepness of FFR within the range of stimulation frequencies (results not shown). Thus the flattening of FFR in EED muscles could not be corrected by β-receptor stimulation.

ET-1 is a potent positive inotropic agent produced in endothelium (38). Conceivably, removal of EE would impair production of ET-1, dampening FFR. We tested this possibility by exposing EED muscles to ET-1 (20–100 nmol/l). ET-1 at 20 nmol/l increased baseline force development but did not change the slope of FFR (Fig. 5*B*). Similarly, the highest ET-1 dose (100 nmol/l) resulted in higher baseline force but did not increase the slope of FFR (results not shown) in EED muscles. Thus neither ISO nor ET-1 alone was able to restore positive FFR staircase.

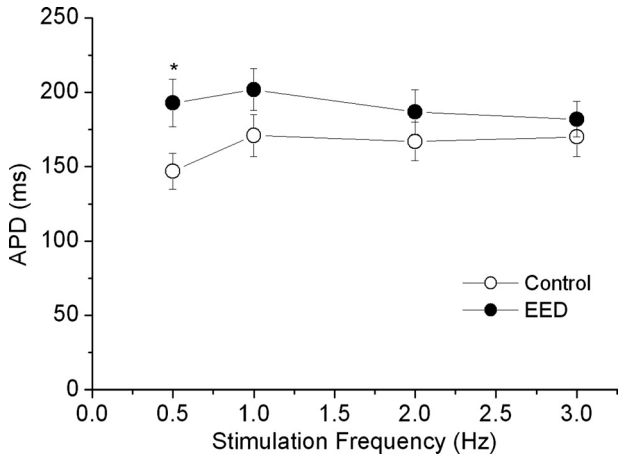

Fig. 4. Effect of EED on action potential duration (APD). The action potential was measured by impaling a microelectrode filled with NaCl (140 mmol/l) into one myocyte in the muscle. $N = 3$; $^*P < 0.05$ by paired *t*-test.

Combination of ISO and ET-1 Restores Positive FFR After EE Removal

In canine trabeculae, low concentrations of the β-agonist norepinephrine unmask ET-1-induced positive inotropic attitude, whereas high doses prevent ET-1 effects (11). Based on this evidence of endothelial-myocardial signaling, we tested whether a combination of ISO and ET-1 could obviate negative FFR in EED muscles.

Both ISO and ET-1 at high concentrations increased baseline forces but blunted FFR in EED muscles (data not shown). Therefore, we tested the combined effects produced by low concentrations of ISO (0.1 nmol/l) and ET-1 (20 nmol/l). When ET-1 was added to the perfusion buffer 10 min after ISO, the combination completely rescued FFR positive slope (Fig. 6*A*). This effect was associated with nearly complete recovery of iCa^{2+} (force: 203 ± 63%; iCa^{2+}: 94 ± 15%, $P < 0.05$ vs. untreated EED, $n = 7$; Fig. 6*B*). In parallel experiments, the combination of ISO and ET-1 did not affect FFR in intact control muscles (Fig. 7*A*). Also, application of ET-1 20 min before ISO did not restore FFR positive slope (Fig. 7*B*), suggesting that a low concentration of a β-agonist exerts a "permissive" effect on ET-1 signaling to restore FFR when EE is absent. Finally, FFR was inhibited by propranolol (30 nmol/l), confirming the involvement of the β_1-adrenergic pathway in positive FFR in intact control muscle (Fig. 7*C*).

Blockade of the PKA or PKC Pathway Abolishes the Recovery of FFR by ISO and ET-1 in EED Muscles

To confirm the involvement of β-receptor and ET-1 receptor in rescuing positive FFR in EED muscles, we studied separate groups of muscles in the presence of β_1-adrenergic and ET-1 pathway blockade. CGP (2 μmol/l), a β_1-adrenergic pathway

Downloaded from www.physiology.org/journal/jappl (071.179.232.088) on January 25, 2020.

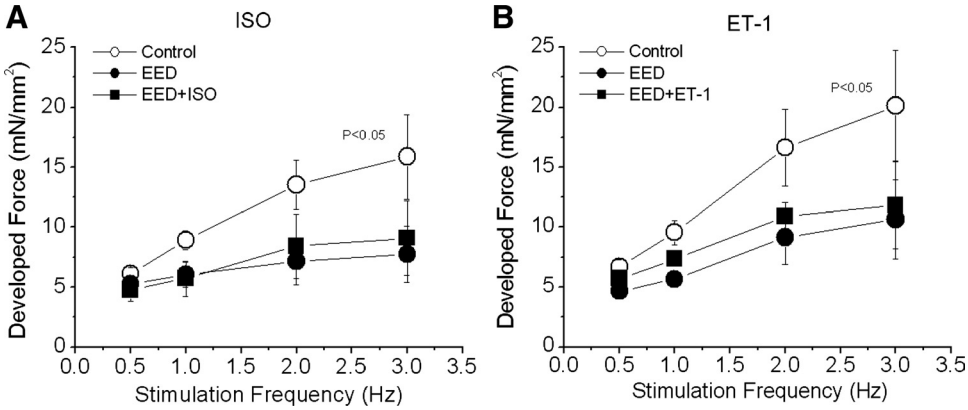

Fig. 5. Pooled data showing the effect of isoproterenol (ISO) or endothelin 1 (ET-1) on the force-frequency relationship (FFR) in rat trabeculae with damaged endocardial endothelium. Trabeculae were intact (control) or endocardial endothelium-denuded (EED). The depressed FFR of the EED trabeculae was not improved by ISO (0.1 nmol/l, $n = 4$, *A*) or by ET-1 (20 nmol/l, $n = 5$, *B*). $P < 0.05$ vs. treated groups by multivariate ANOVA.

blocker (51, 64), increased force development at all stimulation frequencies considered (Fig. 8*A*). However, it abolished the positive FFR induced by combined ISO and ET-1 in EED muscles. CGP per se had no effect in intact EE muscles (data not shown). To confirm the involvement of β_1-PKA signaling, we also tested the effects of the PKA inhibitor H-89 (1 μmol/l) (17). H-89 abolished the action of ISO and ET-1 on FFR in EED muscles (Fig. 8*B*).

In ventricular myocytes, ET-1 acts on membrane ET_A receptors to increase contractility (33). One important step in ET-1 signaling is phospholipase C (PLC)-diacylglycerol-dependent activation of PKC (58). To cement the role of the ET-1-PLC-PKC pathway in FFR, we used the PLC inhibitor neomycin. Neomycin (10 μmol/l) was added to the perfusion buffer after muscles had been treated with 0.1 nmol/l ISO for 15 min. Neomycin did not affect contraction in either intact or EED muscles at baseline. However, it blocked the restoration of FFR in EED muscles by the combination of ISO and ET-1 (Fig. 8*C*) by blunting the increase in iCa^{2+}. High concentrations of neomycin (0.1–0.5 mmol/l) decreased force and abolished the positive FFR in intact control muscles (results not shown). To further demonstrate the involvement of the ET-1-PLC-PKC pathway, we treated EED muscles with the PKC inhibitor staurosporine (10 nmol/l). Like neomycin, staurosporine prevented the restoration of positive FFR by ISO plus ET-1 in these muscles (Fig. 8*D*).

PKA and PKC Activity at Low and High Stimulation Rates in Cardiac Muscles

To strengthen the evidence that both PKA and PKC signaling pathways are involved in the restoration of positive FFR in EED muscles by ISO plus ET-1, we measured the activity of PKA and PKC during stimulation of trabeculae at low (0.5 Hz) and high (3.0 Hz) frequencies. In intact muscles, the ascending slope of the FFR was associated with increases in activity of both PKA and PKC (Fig. 9, *A* and *B*). Removal of EE not only flattened the FFR but also abolished the increases in PKA and PKC activity. As in Fig. 6, combining low concentrations of ISO and ET-1 restored the FFR of EED muscles almost to the level of intact muscle (Fig. 9*C*) and augmented PKA and PKC activity (Fig. 9*D*). The PKA inhibitor H-89 and the PKC inhibitor staurosporine prevented the increase in activity of the respective kinase, retarding the recovery of FFR (Fig. 9, *C* and *D*). Hence, restoration of FFR by the combination of ISO and ET-1 depends on the simultaneous and synergistic activation of PKA and PKC pathways.

DISCUSSION

Here we provide the first direct proof that EE is essential for a fully developed positive FFR in the cardiac muscle. Central to this phenomenon is the synergy between PKA- and PKC-driven signaling that rises in the myocardium proportionally to the increase in the stimulation rate.

Coupling of EE to Cardiomyocytes Impacts FFR

That EE and myocytes actively interact is a well-consolidated fact (9). Myocytes interact with endothelium at two sites, EE (9) and myocardial capillaries. In this study, we chose to investigate the role of EE-myocyte coupling in FFR for three main reasons. First, EE and myocardial capillary endothelium share common features in their effect on myocardial contraction (59). Thus studies of either one could be representative of

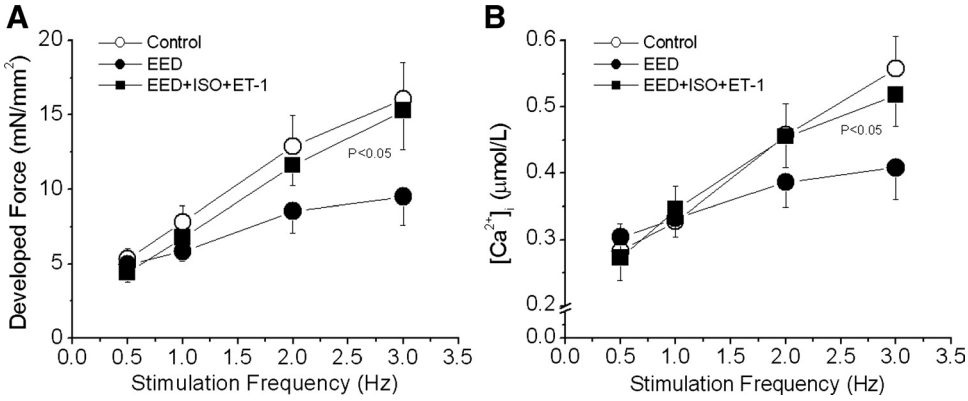

Fig. 6. Pooled data showing the effect of ISO plus ET-1 on the FFR in rat trabeculae with damaged endocardial endothelium. FFR was measured in intact trabeculae (control), endocardial endothelium-denuded trabeculae (EED), and EED trabeculae treated with a low concentration of ISO (0.1 nmol/l) and ET-1 (20 nmol/l). The combination of ISO and ET-1 almost completely restored developed force (*A*) and intracellular Ca^{2+} transients (*B*) to the levels of control trabeculae. $P < 0.05$ vs. EED group by multivariate ANOVA; $n = 7$.

Downloaded from www.physiology.org/journal/jappl (071.179.232.088) on January 25, 2020.

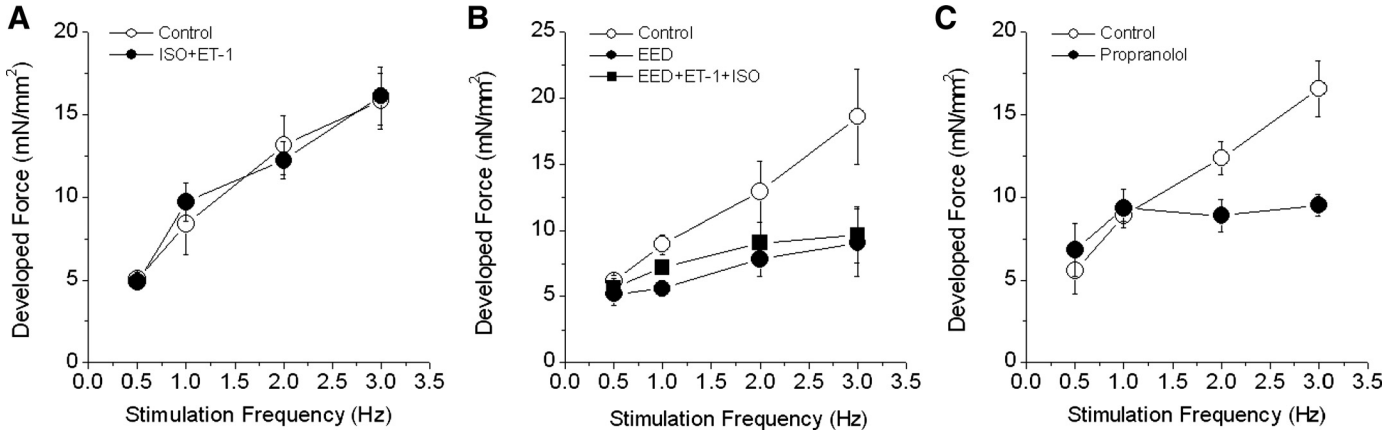

Fig. 7. Effect of ISO, ET-1, and propranolol on the FFR in trabeculae. *A*: combination of ISO and ET-1 had no effect on FFR in intact trabeculae ($n = 4$). *B*: effect of ET-1 plus ISO on FFR in endocardial endothelium-denuded (EED) trabeculae. The muscles were treated with ET-1 (20 nmol/l) for 20 min before ISO (0.1 nmol/l) was added to the perfusion solution. Despite some recovery of force at all test stimulation frequencies, the slope of the FFR was not improved. *C*: propranolol (30 nmol/l) inhibited the FFR, especially at higher stimulation frequencies ($n = 5$).

the other. Second, EE-myocyte coupling can be easily interrupted experimentally without affecting neighboring myocytes. Third, in right ventricle, the extent of EE-myocyte interaction can be as much as 50% of wall thickness because of intense trabeculations. Thus the impact of EE-myocyte coupling alone on right heart contraction can be substantial.

It is well known that at resting rates, endothelial cells influence myocyte contraction via autocrine and paracrine factors such as endothelins (58), NO (49), prostacyclins (45), and angiotensin II (43). However, whether EE influences the positive FFR staircase exhibited by normal cardiac muscle (22) is an unasked question. The central phenomenon accounting for a positive FFR is the frequency-dependent increase in intracellular Ca^{2+} availability during excitation-contraction coupling. The effect, namely greater cytosolic Ca^2 availability, results from enhanced Ca^{2+} entry and SR Ca^{2+} release (20, 55, 57). Consistent with prior studies (22), our results showed a frequency-dependent increase in iCa^{2+} that led to a positive FFR in control muscles that maintain endo-myocyte interactions. In contrast, the FFR became less steep in EED muscles,

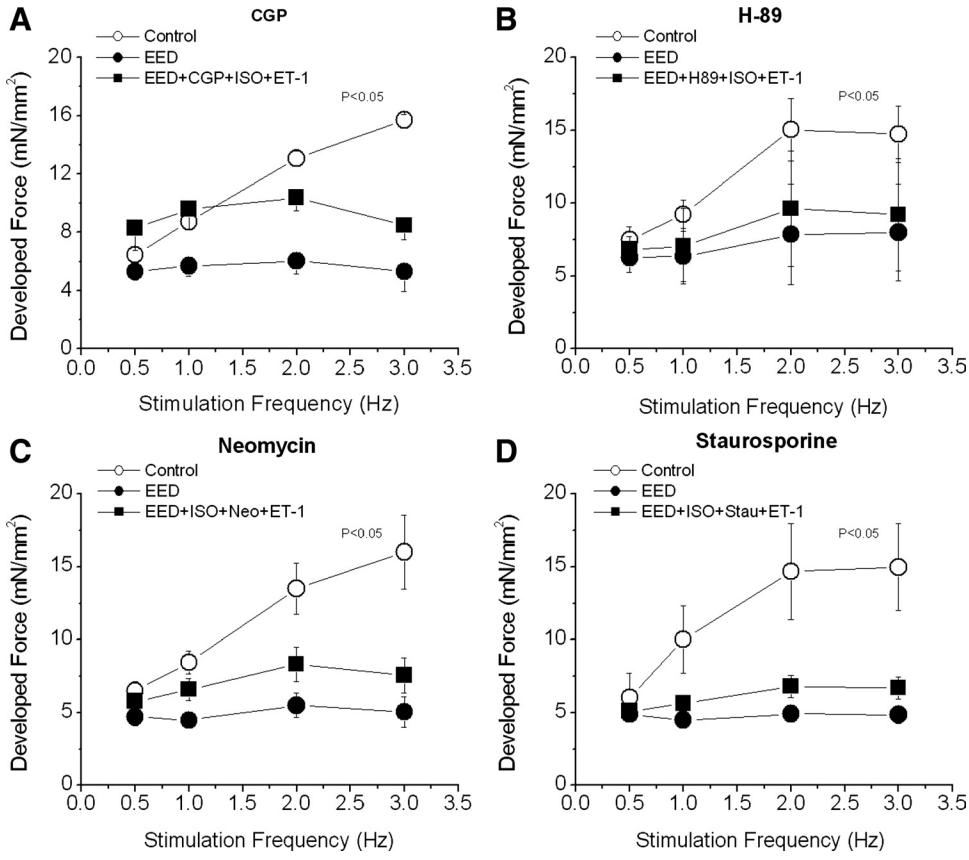

Fig. 8. Effect of adrenergic, PKA, PKC, and PLC blockade on the FFR. FFR was measured in intact trabeculae (control) and in EED trabeculae. *A* and *B*: EED trabeculae were treated with CGP (2 μmol/l), a β_1-adrenergic blocker (*A*), or H-89 (1 μmol/l), a PKA inhibitor (*B*), for 20 min after the endocardial endothelium was selectively damaged. Then ISO (0.1 nmol/l) and ET-1 (20 nmol/l) were added. *C* and *D*: EED muscles were treated with ISO (0.1 nmol/l) for 15 min followed by neomycin (Neo; 10 μmol/l), a PLC inhibitor (*C*), or staurosporine (Stau; 10 nmol/l), a PKC inhibitor (*D*), for 15 min. Then ET-1 (10 nmol/l) was added for 20 min. $P < 0.05$, control vs. other groups by multivariate ANOVA; $n = 3$–5 in each group.

Downloaded from www.physiology.org/journal/jappl (071.179.232.088) on January 25, 2020.

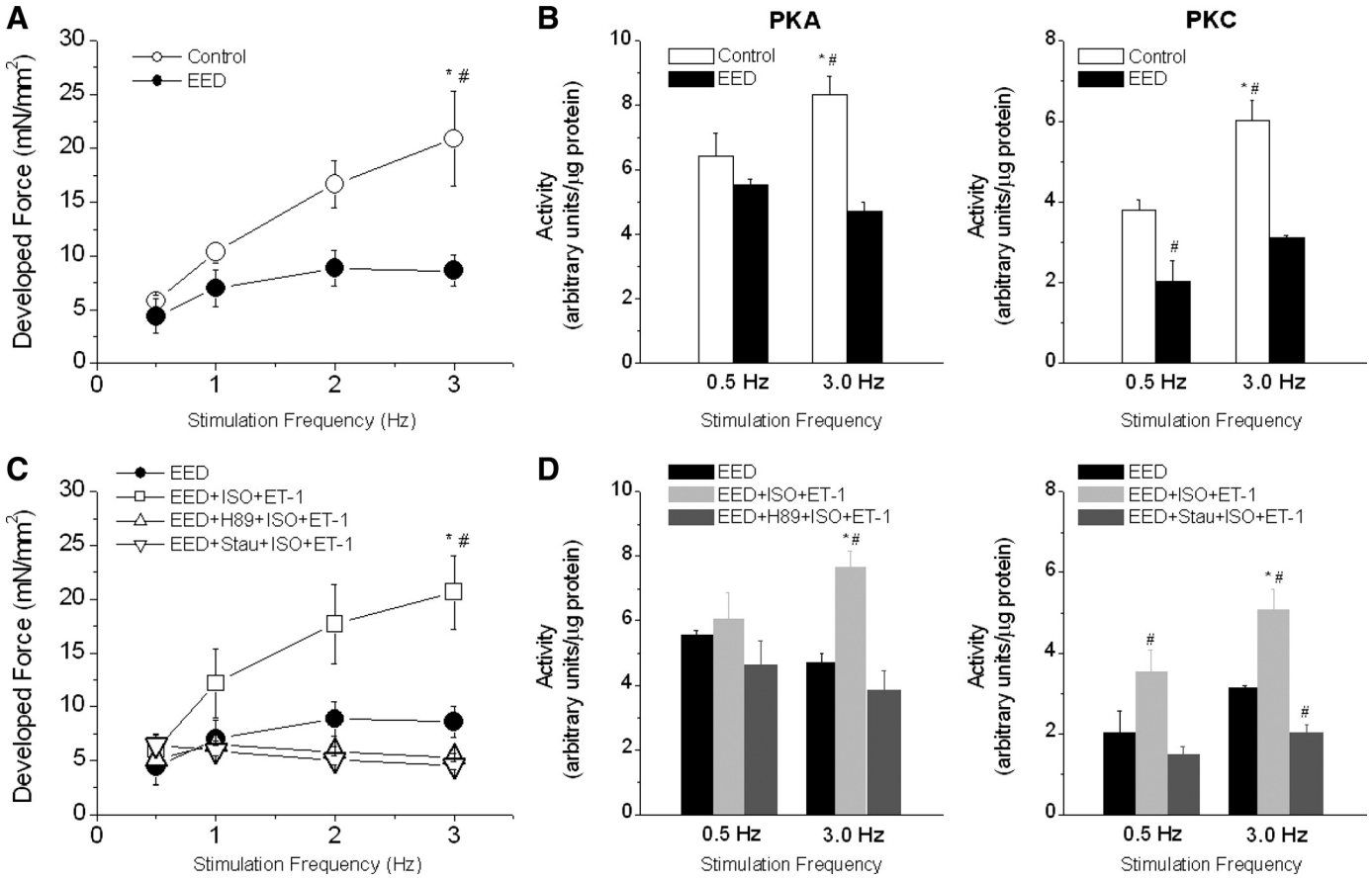

Fig. 9. Association between the FFR and activity levels of PKA and PKC. *A*: effect of stimulation frequency on developed force in control (intact) and EED cardiac muscle. *B*: effect of stimulation frequency on PKA activity and PKC activity in control and EED cardiac muscle (n = 8–12). Frequency-dependent increases in PKA and PKC activity were observed in control but not in EED muscles. *C* and *D*: the combination of ISO (0.1 nmol/l) and ET-1 (10 nmol/l) restored the FFR (*C*) and frequency-dependent increases in PKA and PKC activity (*D*) in EED muscle. However, H-89 blocked the increase in PKA activity and staurosporine blocked the increase in PKC activity (n = 5–8). *$P < 0.05$ vs. 0.5-Hz stimulation frequency; #$P < 0.05$ vs. other groups at the same stimulation frequency.

in which such interactions were disrupted. Furthermore, it is evident from our study that this blunted FFR results from the inability of the excitation-contraction coupling machinery to increase iCa^{2+} as the stimulation frequency increases in these EED muscles (Fig. 3). Therefore, the first main conclusion that can be drawn from our study is that an intact EE is not required for a positive FFR staircase in the cardiac muscle. However, it is essential for a fully developed positive FFR.

Decreased myofilament Ca^{2+} responsiveness may be responsible for the flattening of FFR in EED muscles. However, this mechanism became less prominent at high stimulation rates, during which the frequency-dependent increases in iCa^{2+} were also significantly suppressed. The finding that ET-1, a known myocardial Ca^{2+} sensitizer (62), could not restore FFR in EED muscles also argues against a major role of myofilament desensitization (Fig. 4*B*). It appears that decreased intracellular Ca^{2+} availability is responsible for the blunting of positive FFR in EED muscles.

PKA and PKC Signaling are Implicated in EE-Mediated, Fully Developed FFR Response in the Cardiac Muscle

As discussed above, frequency-dependent SR Ca^{2+} release is limited by disruption of EE-myocyte coupling. It is known that when stimulation rate is increased, SR Ca^{2+} load/uptake (relative to Ca^{2+} extrusion via sarcolemma) increases (1, 3), leading to augmented Ca^{2+} release (20, 55). The SR Ca^{2+}-ATPase is crucial for SR Ca^{2+} loading (24) and is modulated by phospholamban (34). Importantly, β-adrenergic-PKA pathway activation phosphorylates phospholamban and increases SR Ca^{2+} loading and release (6). However, in EED muscles, β_1-adrenergic stimulation alone (either low or high concentration) could not restore the flat FFR response to the positive staircase typical of normal muscle (Fig. 5*A*). Although a high concentration of ISO increased force development significantly in EED muscles at baseline stimulation rate, the positivity of the FFR was still lost. SR Ca^{2+} overload and the overwhelming myofilament desensitization with high β-adrenergic stimulation likely underlay the failure of force to rise when stimulation rate was increased. Only a combination of ISO and ET-1 at low concentrations was able to produce the frequency-dependent increases in iCa^{2+} and restore FFR in EED muscles. This finding suggests that cross-talk occurs between ISO and ET-1 in modulating FFR. Furthermore, such cross-talk is associated with synergistic activation of PKA and PKC (Fig. 9). Apparently, such cross-talk requires subthreshold activations of both PKA and PKC at baseline stimulation frequency as activation of each individually did not produce appreciable effect on force development. As stimulation frequency was

Downloaded from www.physiology.org/journal/jappl (071.179.232.088) on January 25, 2020.

increased, the activity of PKA and PKC increased, resulting in increased iCa^{2+} and a positive FFR. Thus the presence of intact EE and, therefore, EE-myocyte coupling, enables the cross-talk and orchestrate balanced activation of both PKA and PKC pathways to increase iCa^{2+} as stimulation rate is increased. It is currently unknown exactly how PKA and PKC pathways interact to promote SR Ca^{2+} release during positive FFR.

Although individual myocytes alone are able to produce a positive FFR, the presence of EE and EE-myocyte coupling enhances the magnitude of a positive FFR. This enhancement is achieved by maintaining synergistic activation of PKA and PKC via β_1-adrenergic and ET-1 receptors in myocytes. Conceivably, ET-1 receptors are stimulated by ET-1 that is secreted by EE. It is unclear, however, how EE-myocyte coupling stimulates β_1-adrenergic receptors/pathway. Although factors produced by EE that can act directly on β_1-adrenergic receptors have yet to be discovered, two agents (among those known to be involved in EE-myocyte coupling), NO (low concentrations) and prostacyclins, have been shown to increase cAMP production (8, 44). Low concentrations of NO (corresponding to levels generated endogenously by endothelial cell NO synthase) produce low levels of cGMP, which inhibit phosphodiesterase III and elevate cAMP levels (61). NO itself does not have a measurable effect on FFR (12). Prostaglandin E increases cAMP levels in the cytosol (30). The consequences of prostaglandin-induced increases in cellular cAMP content are still the focus of many investigators. Whether NO and/or prostaglandins are involved in mediating FFR by EE-myocyte coupling remains as an interesting future study.

Neuregulin (NRG)-1-ErbB signaling has recently been recognized to play a crucial role in maintaining normal function of the heart (18) and may be involved in regulating FFR, especially given that EE cells are the major source of NRG (36). The NRG-1-ErbB pathway activates the PI3K-Akt system, which maintains iCa^{2+} (28). Thus the flattened FFR could be due to loss of EE NRG, and ET-1 + ISO might restore a positive FFR by transactivating ErbB receptors (16, 47). Elucidating the role of the NRG-1-ErbB pathway in EE-myocyte coupling remains as an appealing project for future investigations.

Limitations

We did not investigate the interaction between coronary endothelium and myocytes directly in this study. Therefore, extrapolation of our data to the left ventricle, where myocardial capillary endothelium is predominant, may be limited owing to morphological and functional differences (9). Nevertheless, prior studies have demonstrated that selectively disabling coronary endothelium produces an effect similar to that of removing EE in isolated cardiac muscles (37). Another limitation of the study is that we determined only whole tissue PKA/PKC activity, thus offering little insight into molecular mechanisms for the cross-talk between PKA and PKC, which remains to be studied in future investigations. For example, the presence of kinase-anchoring proteins for PKA (19) and the existence of PKC isoenzymes and associated receptors (31) compartmentalize PKA and PKC signaling pathways. Studies of the involvement of these proteins would provide important information on the cross-talk between PKA and PKC pathways in modulating FFR. Finally, the status of phosphorylation of contractile proteins in the trabeculae under varied experimental conditions was not examined in this study. Such challenging experiments would substantiate our study.

Pragmatic Implications and Conclusions

FFR is an important intrinsic regulatory property of cardiac muscle. FFR is also modulated by a number of receptor-mediated signal transduction processes. To our knowledge, our study is the first to highlight the ability of endothelial-myocyte coupling to modulate FFR. The translational implications are significant, especially for chronic cardiac disease conditions such as congestive heart failure (CHF). Cardiac endothelial dysfunction is closely involved in pathogenesis and progress of heart failure (4, 5). For instance, endothelial dysfunction causes abnormal coronary vasoconstriction in rats with CHF (54). Additionally, EE has been shown to be damaged in rat hearts after cardiac infarction (52). In particular, muscles from failing hearts behaved like control muscles with EE damage (52). A negative FFR staircase is a prominent hallmark of CHF. Given its critical role in modulating FFR, altered EE-myocyte coupling could play an important role in the pathogenesis of negative FFR in heart failure.

In conclusion, removal of EE or disrupting EE-myocyte coupling negatively impacts FFR. The mechanism for EE-myocyte coupling to maintain a positive FFR involves synergistic activations of PKA and PKC, indicating balanced cross-talk between the β_1-adrenergic-PKA pathway and the ET-1-PKC pathway. Although the molecular nature for the cross-talk between the two pathways remains to be identified, our study highlights the crucial role of EE in FFR and links altered EE-myocyte coupling to the negative FFR in heart failure states.

GRANTS

This study was supported in part by National Institutes of Health Grants HL63038 (A.M.M) and HL091923 (N. P), by American Heart Association AHA0855439E (W.D.G) and AHA-12SDG140008 (G.R.-C), and by Lawrence J. and Florence A. DeGeorge Charitable Trust (G.R.-C).

DISCLOSURES

No conflicts of interest, financial or otherwise, are declared by the author(s).

AUTHOR CONTRIBUTIONS

Author contributions: X.S., Z.T., X.Z., Y.T., K.L.G., and W.D.G. performed experiments; X.S., Z.T., X.Z., Y.T., G.R.-C., K.L.G., and W.D.G. analyzed data; X.S., Z.T., G.R.-C., K.L.G., and W.D.G. prepared figures; X.S., Z.T., and W.D.G. drafted manuscript; X.S., Z.T., X.Z., Y.T., B.Y., X.W., G.R.-C., A.M.M., N.P., and W.D.G. approved final version of manuscript; X.W., B.Y., G.R.-C., A.M.M., K.L.G., N.P., and W.D.G. interpreted results of experiments; X.W., G.R.-C., A.M.M., N.P., and W.D.G. edited and revised manuscript; W.D.G. conception and design of research.

REFERENCES

1. **Antoons G, Mubagwa K, Nevelsteen I, Sipido KR.** Mechanisms underlying the frequency dependence of contraction and [Ca(2+)](i) transients in mouse ventricular myocytes. *J Physiol* 543: 889–898, 2002.
2. **Backx PH, Gao WD, Azan-Backx MD, Marban E.** Mechanism of force inhibition by 2,3-butanedione monoxime in rat cardiac muscle: roles of $[Ca^{2+}]_i$ and cross-bridge kinetics. *J Physiol* 476: 487–500, 1994.
3. **Baudet S, Do E, Noireaud J, Le Marec H.** Alterations in the force-frequency relationship by tert-butylbenzohydroquinone, a putative SR Ca^{2+} pump inhibitor, in rabbit and rat ventricular muscle. *Br J Pharmacol* 117: 258–267, 1996.

Downloaded from www.physiology.org/journal/jappl (071.179.232.088) on January 25, 2020.

4. **Bauersachs J, Schafer A.** Endothelial dysfunction in heart failure: mechanisms and therapeutic approaches. *Curr Vasc Pharmacol* 2: 115–124, 2004.
5. **Bauersachs J, Widder JD.** Endothelial dysfunction in heart failure. *Pharmacol Rep* 60: 119–126, 2008.
6. **Bers DM.** Cardiac excitation-contraction coupling. *Nature* 415: 198–205, 2002.
7. **Bluhm WF, Kranias EG, Dillmann WH, Meyer M.** Phospholamban: a major determinant of the cardiac force-frequency relationship. *Am J Physiol Heart Circ Physiol* 278: H249–H255, 2000.
8. **Bos CL, Richel DJ, Ritsema T, Peppelenbosch MP, Versteeg HH.** Prostanoids and prostanoid receptors in signal transduction. *Int J Biochem Cell Biol* 36: 1187–1205, 2004.
9. **Brutsaert DL.** Cardiac endothelial-myocardial signaling: its role in cardiac growth, contractile performance, and rhythmicity. *Physiol Rev* 83: 59–115, 2003.
10. **Brutsaert DL, Meulemans AL, Sipido KR, Sys SU.** Effects of damaging the endocardial surface on the mechanical performance of isolated cardiac muscle. *Circ Res* 62: 358–366, 1988.
11. **Chu L, Takahashi R, Norota I, Miyamoto T, Takeishi Y, Ishii K, Kubota I, Endoh M.** Signal transduction and Ca^{2+} signaling in contractile regulation induced by crosstalk between endothelin-1 and norepinephrine in dog ventricular myocardium. *Circ Res* 92: 1024–1032, 2003.
12. **Cotton JM, Kearney MT, MacCarthy PA, Grocott-Mason RM, McClean DR, Heymes C, Richardson PJ, Shah AM.** Effects of nitric oxide synthase inhibition on basal function and the force-frequency relationship in the normal and failing human heart in vivo. *Circulation* 104: 2318–2323, 2001.
13. **Dai T, Ramirez-Correa G, Gao WD.** Apelin increases contraction in failing cardiac muscle. *Eur J Pharmacol* 553: 222–228, 2006.
14. **Dai T, Tian Y, Tocchetti CG, Katori T, Murphy AM, Kass DA, Paolocci N, Gao WD.** Nitroxyl increases force development in rat cardiac muscle. *J Physiol* 580: 951–960, 2007.
15. **Daniels MC, Fedida D, Lamont C, ter Keurs HE.** Role of the sarcolemma in triggered propagated contractions in rat cardiac trabeculae. *Circ Res* 68: 1408–1421, 1991.
16. **Daub H, Weiss FU, Wallasch C, Ullrich A.** Role of transactivation of the EGF receptor in signalling by G-protein-coupled receptors. *Nature* 379: 557–560, 1996.
17. **Davies SP, Reddy H, Caivano M, Cohen P.** Specificity and mechanism of action of some commonly used protein kinase inhibitors. *Biochem J* 351: 95–105, 2000.
18. **De Keulenaer GW, Doggen K, Lemmens K.** The vulnerability of the heart as a pluricellular paracrine organ: lessons from unexpected triggers of heart failure in targeted ErbB2 anticancer therapy. *Circ Res* 106: 35–46.
19. **Edwards AS, Scott JD.** A-kinase anchoring proteins: protein kinase A and beyond. *Curr Opin Cell Biol* 12: 217–221, 2000.
20. **Eisner DA, Choi HS, Diaz ME, O'Neill SC, Trafford AW.** Integrative analysis of calcium cycling in cardiac muscle. *Circ Res* 87: 1087–1094, 2000.
21. **Endoh M.** Changes in intracellular Ca^{2+} mobilization and Ca^{2+} sensitization as mechanisms of action of physiological interventions and inotropic agents in intact myocardial cells. *Jpn Heart J* 39: 1–44, 1998.
22. **Endoh M.** Force-frequency relationship in intact mammalian ventricular myocardium: physiological and pathophysiological relevance. *Eur J Pharmacol* 500: 73–86, 2004.
23. **Ezzaher A, el Houda Bouanani N, Crozatier B.** Force-frequency relations and response to ryanodine in failing rabbit hearts. *Am J Physiol Heart Circ Physiol* 263: H1710–H1715, 1992.
24. **Frank KF, Bolck B, Erdmann E, Schwinger RH.** Sarcoplasmic reticulum Ca^{2+}-ATPase modulates cardiac contraction and relaxation. *Cardiovasc Res* 57: 20–27, 2003.
25. **Gao WD, Backx PH, Azan-Backx M, Marban E.** Myofilament Ca^{2+} sensitivity in intact versus skinned rat ventricular muscle. *Circ Res* 74: 408–415, 1994.
26. **Gao WD, Liu Y, Mellgren R, Marban E.** Intrinsic myofilament alterations underlying the decreased contractility of stunned myocardium. A consequence of Ca^{2+}-dependent proteolysis? *Circ Res* 78: 455–465, 1996.
27. **Gao WD, Perez NG, Marban E.** Calcium cycling and contractile activation in intact mouse cardiac muscle. *J Physiol* 507: 175–184, 1998.
28. **Graves BM, Simerly T, Li C, Williams DL, Wondergem R.** Phosphoinositide-3-kinase/akt-dependent signaling is required for maintenance of $[Ca^{2+}]_i$, I_{Ca}, and Ca^{2+} transients in HL-1 cardiomyocytes. *J Biomed Sci* 19: 59.
29. **Hashimoto K, Perez NG, Kusuoka H, Baker DL, Periasamy M, Marban E.** Frequency-dependent changes in calcium cycling and contractile activation in SERCA2a transgenic mice. *Basic Res Cardiol* 95: 144–151, 2000.
30. **Hayes JS, Brunton LL, Mayer SE.** Selective activation of particulate cAMP-dependent protein kinase by isoproterenol and prostaglandin E1. *J Biol Chem* 255: 5113–5119, 1980.
31. **Hool LC.** Protein kinase C isozyme selective peptides—a current view of what they tell us about location and function of isozymes in the heart. *Curr Pharm Des* 11: 549–559, 2005.
32. **Janssen PM, Stull LB, Marban E.** Myofilament properties comprise the rate-limiting step for cardiac relaxation at body temperature in the rat. *Am J Physiol Heart Circ Physiol* 282: H499–H507, 2002.
33. **Kelso EJ, McDermott BJ, Silke B, Spiers JP.** Endothelin(A) receptor subtype mediates endothelin-induced contractility in left ventricular cardiomyocytes isolated from rabbit myocardium. *J Pharmacol Exp Ther* 294: 1047–1052, 2000.
34. **Koss KL, Kranias EG.** Phospholamban: a prominent regulator of myocardial contractility. *Circ Res* 79: 1059–1063, 1996.
35. **Layland J, Kentish JC.** Positive force- and $[Ca^{2+}]_i$-frequency relationships in rat ventricular trabeculae at physiological frequencies. *Am J Physiol Heart Circ Physiol* 276: H9–H18, 1999.
36. **Lemmens K, Segers VF, Demolder M, De Keulenaer GW.** Role of neuregulin-1/ErbB2 signaling in endothelium-cardiomyocyte cross-talk. *J Biol Chem* 281: 19469–19477, 2006.
37. **Li K, Rouleau JL, Calderone A, Andries JL, Brutsaert DL.** Effects of dysfunctional vascular endothelium on myocardial performance in isolated papillary muscles. *Circ Res* 72: 768–777, 1993.
38. **Li K, Stewart DJ, Rouleau JL.** Myocardial contractile actions of endothelin-1 in rat and rabbit papillary muscles. Role of endocardial endothelium. *Circ Res* 69: 301–312, 1991.
39. **Maier LS, Bers DM.** Calcium, calmodulin, and calcium-calmodulin kinase II: heartbeat to heartbeat and beyond. *J Mol Cell Cardiol* 34: 919–939, 2002.
40. **Maier LS, Bers DM, Pieske B.** Differences in Ca^{2+}-handling and sarcoplasmic reticulum Ca^{2+}-content in isolated rat and rabbit myocardium. *J Mol Cell Cardiol* 32: 2249–2258, 2000.
41. **McClellan G, Weisberg A, Rose D, Winegrad S.** Endothelial cell storage and release of endothelin as a cardioregulatory mechanism. *Circ Res* 75: 85–96, 1994.
42. **Mebazaa A, Mayoux E, Maeda K, Martin LD, Lakatta EG, Robotham JL, Shah AM.** Paracrine effects of endocardial endothelial cells on myocyte contraction mediated via endothelin. *Am J Physiol Heart Circ Physiol* 265: H1841–H1846, 1993.
43. **Meulemans AL, Andries LJ, Brutsaert DL.** Does endocardial endothelium mediate positive inotropic response to angiotensin I and angiotensin II? *Circ Res* 66: 1591–1601, 1990.
44. **Mohan P, Brutsaert DL, Paulus WJ, Sys SU.** Myocardial contractile response to nitric oxide and cGMP. *Circulation* 93: 1223–1229, 1996.
45. **Mohan P, Brutsaert DL, Sys SU.** Myocardial performance is modulated by interaction of cardiac endothelium derived nitric oxide and prostaglandins. *Cardiovasc Res* 29: 637–640, 1995.
46. **Morgan JP, Erny RE, Allen PD, Grossman W, Gwathmey JK.** Abnormal intracellular calcium handling, a major cause of systolic and diastolic dysfunction in ventricular myocardium from patients with heart failure. *Circulation* 81: III21–III32, 1990.
47. **Noma T, Lemaire A, Naga Prasad SV, Barki-Harrington L, Tilley DG, Chen J, Le Corvoisier P, Violin JD, Wei H, Lefkowitz RJ, Rockman HA.** Beta-arrestin-mediated beta1-adrenergic receptor transactivation of the EGFR confers cardioprotection. *J Clin Invest* 117: 2445–2458, 2007.
48. **Ono K, Tsujimoto G, Sakamoto A, Eto K, Masaki T, Ozaki Y, Satake M.** Endothelin-A receptor mediates cardiac inhibition by regulating calcium and potassium currents. *Nature* 370: 301–304, 1994.
49. **Palmer RM, Ferrige AG, Moncada S.** Nitric oxide release accounts for the biological activity of endothelium-derived relaxing factor. *Nature* 327: 524–526, 1987.
50. **Penna C, Rastaldo R, Mancardi D, Cappello S, Pagliaro P, Westerhof N, Losano G.** Effect of endothelins on the cardiovascular system. *J Cardiovasc Med (Hagerstown)* 7: 645–652, 2006.
51. **Perez-Schindler J, Philp A, Baar K, Hernandez-Cascales J.** Regulation of contractility and metabolic signaling by the beta2-adrenergic receptor in rat ventricular muscle. *Life Sci* 88: 892–897, 2011.

Downloaded from www.physiology.org/journal/jappl (071.179.232.088) on January 25, 2020.

52. **Qi XL, Stewart DJ, Gosselin H, Azad A, Picard P, Andries L, Sys SU, Brutsaert DL, Rouleau JL.** Improvement of endocardial and vascular endothelial function on myocardial performance by captopril treatment in postinfarct rat hearts. *Circulation* 100: 1338–1345, 1999.
53. **Rossman EI, Petre RE, Chaudhary KW, Piacentino V, 3rd Janssen PM, Gaughan JP, Houser SR, Margulies KB.** Abnormal frequency-dependent responses represent the pathophysiologic signature of contractile failure in human myocardium. *J Mol Cell Cardiol* 36: 33–42, 2004.
54. **Schafer A, Fraccarollo D, Pfortsch S, Loch E, Neuser J, Vogt C, Bauersachs J.** Clopidogrel improves endothelial function and NO bioavailability by sensitizing adenylyl cyclase in rats with congestive heart failure. *Basic Res Cardiol* 106: 485–494, 2011.
55. **Shannon TR, Bers DM.** Integrated Ca^{2+} management in cardiac myocytes. *Ann NY Acad Sci* 1015: 28–38, 2004.
56. **Smith JA, Shah AM, Lewis MJ.** Factors released from endocardium of the ferret and pig modulate myocardial contraction. *J Physiol* 439: 1–14, 1991.
57. **Stemmer P, Akera T.** Concealed positive force-frequency relationships in rat and mouse cardiac muscle revealed by ryanodine. *Am J Physiol Heart Circ Physiol* 251: H1106–H1110, 1986.
58. **Sugden PH.** An overview of endothelin signaling in the cardiac myocyte. *J Mol Cell Cardiol* 35: 871–886, 2003.
59. **Sys SU, De Keulenaer GW, Brutsaert DL.** Physiopharmacological evaluation of myocardial performance: how to study modulation by cardiac endothelium and related humoral factors? *Cardiovasc Res* 39: 136–147, 1998.
60. **Taylor DG, Parilak LD, LeWinter MM, Knot HJ.** Quantification of the rat left ventricle force and Ca^{2+}-frequency relationships: similarities to dog and human. *Cardiovasc Res* 61: 77–86, 2004.
61. **Vila-Petroff MG, Younes A, Egan J, Lakatta EG, Sollott SJ.** Activation of distinct cAMP-dependent and cGMP-dependent pathways by nitric oxide in cardiac myocytes. *Circ Res* 84: 1020–1031, 1999.
62. **Wang J, Morgan JP.** Endocardial endothelium modulates myofilament Ca^{2+} responsiveness in aequorin-loaded ferret myocardium. *Circ Res* 70: 754–760, 1992.
63. **Wang JX, Paik G, Morgan JP.** Endothelin 1 enhances myofilament Ca^{2+} responsiveness in aequorin-loaded ferret myocardium. *Circ Res* 69: 582–589, 1991.
64. **Xiao RP, Avdonin P, Zhou YY, Cheng H, Akhter SA, Eschenhagen T, Lefkowitz RJ, Koch WJ, Lakatta EG.** Coupling of beta2-adrenoceptor to Gi proteins and its physiological relevance in murine cardiac myocytes. *Circ Res* 84: 43–52, 1999.

Downloaded from www.physiology.org/journal/jappl (071.179.232.088) on January 25, 2020.